Journal of Pathology
J Pathol 2005; **205**: 194–205
Published online in Wiley InterScience (www.interscience.wiley.com). **DOI:** 10.1002/path.1697

Review Article

Advances in imaging mouse tumour models *in vivo*

Scott K Lyons*
Oncology Department, Xenogen Corporation, Alameda, CA 94501, USA

**Correspondence to: Scott K Lyons, Oncology Department, Xenogen Corporation, 860 Atlantic Avenue, Alameda, CA 94501, USA.*
E-mail: scott.lyons@xenogen.com

Received: 5 October 2004
Accepted: 17 October 2004

Abstract

Significant progress has been made recently in the variety of ways that cancer can be non-invasively imaged in murine tumour models. The development and continued refinement of specialized hardware for an array of small animal imaging methodologies are only partly responsible. So too has been the development of new imaging techniques and materials that enable specific, highly sensitive and quantitative measurement of a wide range of tumour-related parameters. Included amongst these new materials are imaging probes that selectively accumulate in tumours, or that become activated by tumour-specific molecules *in vivo*. Other tumour imaging strategies have been developed that rely upon the detection of reporter transgene expression *in vivo*, and these too have made a significant impact on both the versatility and the specificity of tumour imaging in living mice. The biological implications resulting from these latest advances are presented here, with particular emphasis on those associated with MRI, PET, SPECT, BLI, and fluorescence-based imaging modalities. Taken together, these advances in tumour imaging are set to have a profound impact on our basic understanding of *in vivo* tumour biology and will radically alter the application of mouse tumour models in the laboratory.

Keywords: imaging; tumour; mouse model; non-invasive

Introduction

Mouse tumour models have proven to be instrumental tools for furthering our understanding of human cancer. The best mouse models are able to accurately recapitulate many aspects of human tumour physiology such as angiogenesis, tumour–stromal interaction, and hormone dependency. Aspects that underlie the molecular basis of human cancer are also well addressed and mouse models have provided an essential means with which to elucidate the involvement and *in vivo* effects of various genetic lesions in tumourigenesis, tumour progression, and metastasis [1–5]. Beyond advancing our knowledge of basic cancer biology, mouse tumour models also comprise a stringent means with which to preclinically evaluate the *in vivo* efficacy of new therapeutic intervention strategies [6–9], and to characterize factors that influence chemoresistance [10,11].

Xenograft and transgenic mouse models of cancer have traditionally been somewhat of a 'black-box' with respect to all of these advances in our basic understanding of cancer biology. The direct measurement of most meaningful biological parameters (such as the effects of a drug on tumour proliferation or apoptosis rate) has only been achievable via invasive end-point procedures that are both subject- and labour-intensive.

Recent advances within the field of molecular and cellular imaging have now begun to revolutionize the manner with which mouse cancer models are utilized in the laboratory. Through the application of a suite of imaging techniques and reagents, it is now possible for researchers to non-invasively measure a broad range of tumour-relevant parameters at both the cellular and the molecular level. Furthermore, as measurements can be taken at serial time points from the same individual subject, these parameters can be observed dynamically with relative ease. Studies that examine tumour response to therapeutic intervention are now also able to achieve statistical significance using far smaller cohorts of experimental animals, as tumour cell physiology and tumour burden can be accurately determined pre- and post-therapy without assumption.

The aim of this review is to summarize how recent developments in the field of small animal imaging have advanced our understanding of *in vivo* tumour biology. Particular emphasis has been placed on magnetic resonance imaging (MRI), positron emission tomography (PET), single photon emission computed tomography (SPECT), bioluminescence imaging (BLI), and fluorescence imaging, since these approaches have had the most significant impact on mouse tumour model research in recent years. In an effort to focus primarily on the biological implications of these advances, a working knowledge of the basic physics under-pinning each of the individual imaging modalities has been assumed. This information has been covered comprehensively in several other recent reviews, however, should further background be desired [12,13].

Not all imaging modalities are created equal

To better appreciate the latest advances relating to imaging tumours in mice, it is helpful to first consider the various strengths and limitations associated with each individual imaging approach. Table 1 lists the most commonly used small animal imaging modalities along with an outline of the main advantages and disadvantages associated with each.

It should be noted that certain imaging approaches are better suited for specific applications over others. For example, tomographic approaches capable of providing a high degree of spatial resolution, such as computed tomograhy (CT) and MRI, are well suited for tumour phenotyping and anatomical reconstruction of tissues. In comparison, highly sensitive approaches such as PET and BLI are better suited for monitoring tumour cell burden, cellular metabolism, and molecular interactions *in vivo*. Imaging approaches reliant on γ- and X-ray detection are less well suited for frequent imaging schedules, however, as the subject becomes exposed to cumulatively significant doses of radiation. Also, the financial cost of imaging hardware and consumable reagents varies significantly between modalities, as does the relative amount of expertise required for optimal hardware operation.

As no single imaging modality can yet provide all favourable features, multi-modal imaging has become an increasingly common means to utilize and combine the strengths of different approaches in one study. For example, combination PET/CT scanners have recently been developed for imaging mice with the intention of marrying the high sensitivity and high spatial resolution associated with each individual technique [14]. Similarly, MRI and BLI have been employed together to achieve anatomical resolution of tumour structure concurrently with a measure of the distribution and extent of therapeutic gene expression following viral delivery [15]. Other groups have also recently reported the development of tri-fusion reporter transgenes intended for the purpose of multi-modal imaging. When expressed in cells, these transgenes make a single fusion protein composed of luciferase, fluorescent protein, and HSV-TK elements, thereby enabling the researcher to image the cell by either BLI, fluorescence, or PET imaging [16,17]. The rationale behind such an approach is that PET can provide

Table 1. Comparison chart of the main imaging modalities commonly used to image tumours in mice. The main advantages and disadvantages associated with each have been listed. Information partly sourced from refs 12 and 13, as well as other references listed in the main text

Modality (and basis)	Reagents	Resolution and time	Main advantages	Main disadvantages
PET (high-energy γ rays)	^{18}F, ^{11}C, ^{13}N, ^{15}O labelled probes or substrates for reporter transgenes (eg HSV-TK)	1–2 mm; min	High sensitivity; provides quantitative measure of tumour cell metabolism; variety of probes and strategies confers a high degree of versatility	Cyclotron required to generate short-lived radioisotopes; low resolution; unincorporated substrate can increase noise
SPECT (low-energy γ-rays)	^{99m}Tc, ^{111}In, ^{125}I labelled probes	1–2 mm; min	Multiple probes can be detected simultaneously; radioisotopes have longer half-lives than those used in PET	Between 10- and 100-fold less sensitive than PET
MRI (radiowaves)	Paramagnetic cation probes (for contrast enhancement)	25–100 μm; min to h	High spatial resolution; provides both anatomical detail and functional information	Low sensitivity, long acquisition and image process times, so relatively low throughput
CT (X-rays)	Iodine (for contrast enhancement)	50 μm; min	Morphological detection of tumours and metastases in lung and bone	Relatively poor soft-tissue contrast
BLI (visible light)	Luciferase and substrate (Firefly luc: luciferin, *Renilla* luc: coelenterazine)	1–10 mm—dependent on tissue depth; s to min	High sensitivity; provides relative measure of cell viability or cell function; high throughput; transgene-based approach confers versatility	Low anatomic resolution; light emission prone to attenuation with increased tissue depth
Whole-body fluorescence imaging (visible and near-infrared light)	Fluorescent proteins, fluorescent dyes, and quantum dots (CdSe or CdTe nanocrystals)	1–10 mm—dependent on tissue depth; s to min	Multiple reporter wavelengths enables multiplex imaging; highly compatible with a range of *ex vivo* analysis methodologies; transgene-based approach confers versatility	Excitation and emission light <600 nm prone to attenuation with increased tissue depth; autofluorescence of non-labelled cells increases noise
Intra-vital microscopy (visible and near-infrared light)	Fluorescent proteins, fluorescent dyes, and quantum dots	Single cell; min	Microscopic resolution; potential for multiplex imaging; enables real-time imaging and tracking of labelled cell populations	Surgery required to implant tissue window; small field of view; limited to relatively superficial tissues
Ultrasound (high-frequency sound)	Microbubbles (for contrast enhancement)	50 μm; min	Images morphology and physiology of tissue relatively close to the surface of the mouse in real time	Limited ability to image through bone or lungs

tomographic information to non-invasively identify the deep-tissue origin of signal, BLI offers sensitive and high-throughput imaging for longitudinal analyses, and fluorescence imaging can facilitate either *in vivo* imaging or *ex vivo* analyses of labelled cells in fresh-tissue biopsy or cryosection.

Advances in imaging through transgene-based approaches

Many recent advances associated with imaging tumours in small animals have arisen from the application of reporter transgenes. Such approaches are particularly attractive to researchers as the principles governing the generation of transgene-expressing tumour cells or transgenic mice are well established. Furthermore, the number of validated strategies to temporally and spatially regulate transgene expression in mice confers great versatility and enables the non-invasive measurement of a wide range of biological parameters with excellent tumour specificity.

The detection and measurement of luciferase activity (BLI), fluorescent protein excitation (fluorescence imaging), and HSV-TK activity (PET) are among the most commonly employed transgene-based approaches for imaging in mice. Tumour cells can also be engineered to express transferrin receptor to enhance the uptake of an MRI contrast agent [18]. And even LacZ activity, traditionally used as a histological marker in fresh tissue, can now be detected non-invasively via fluorescence [19] or MRI imaging [20]. A variety of strategies have been used to regulate reporter transgene expression (illustrated in Figure 1) and so consequently image many diverse aspects of tumour biology (summarized in Table 2).

Constitutive transgene expression [Figure 1 (I.i)] has been the most extensively employed strategy for *in vivo* imaging in mice to date. This approach has been applied to evaluate the efficacy of therapeutic intervention using tumour xenograft cell lines [21], for monitoring tumour–stroma interactions [22], and for monitoring the efficiency and tumour specificity of *in vivo* gene therapy studies [16]. Spatially restricted [tissue-specific; Figure 1 (I.ii)] and temporally/physiologically restricted reporter transgene expression [inducible; Figure 1 (I.iii)] strategies have also been extensively employed to image tumours in mice. Tissue-specific promoters have been used to image the specificity of virus-mediated gene delivery [23], as well as to visualize spontaneous tumourigenesis arising from a conditional mouse cancer model [24]. Inducible reporter transgene expression has proven an effective means with which to image certain aspects of *in vivo* tumour physiology, such as hypoxia or genotoxic stress [25,26].

Table 2. Summary chart of transgenic imaging strategies and common applications as depicted in Figure 1

Approach	Figure 1	Common applications	Examples	Modalities used
Constitutive transgene expression	(I.i)	Label and determine xenograft model tumour cell burden Evaluate drug efficacy Evaluate efficiency of virally-mediated gene delivery	CMV, SV40, EF-1α, and β-actin promoters	M, P, O
Tissue-specific transgene expression	(I.ii)	Label and determine xenograft and transgenic model tumour cell burden Evaluate drug efficacy Evaluate efficiency and specificity of virally-mediated gene delivery	POMC, PSA promoters	M, P, O
Inducible transgene expression	(I.iii)	Functional label for xenograft and transgenic tumour models Non-invasively monitor angiogenesis, hypoxia, genotoxic stress, etc	VEGF, HIF-1α, COX-2, p53-responsive promoters	P, O
TSTA	(II)	Boost transgene expression in specific cell types following virally-mediated gene delivery	Modified PSA promoter	P, O
Conditional transgene expression	(III)	Functionally report Cre-mediated recombination and tumourigenesis in conditional cancer models	Cre/loxP-dependent reporter allele	P, O
Reporter fusion protein	(IV)	Functional reporter of tumour cell physiology Highly specific *in vivo* drug efficacy screen	Apoptosis, proteasome and cell-cycle-dependent reporter expression	O
Protein–protein dependent transcription	(V)	Monitor protein–protein interaction	p53–T-antigen-dependent reporter expression	P, O
Protein–protein dependent transcription	(VI)	Monitor protein–protein interaction	Split luciferase reporters	O

TSTA = two-step transcriptional amplification; M = magnetic resonance imaging; P = PET or SPECT imaging; O = optical imaging, which includes both bioluminescence and fluorescence imaging techniques.

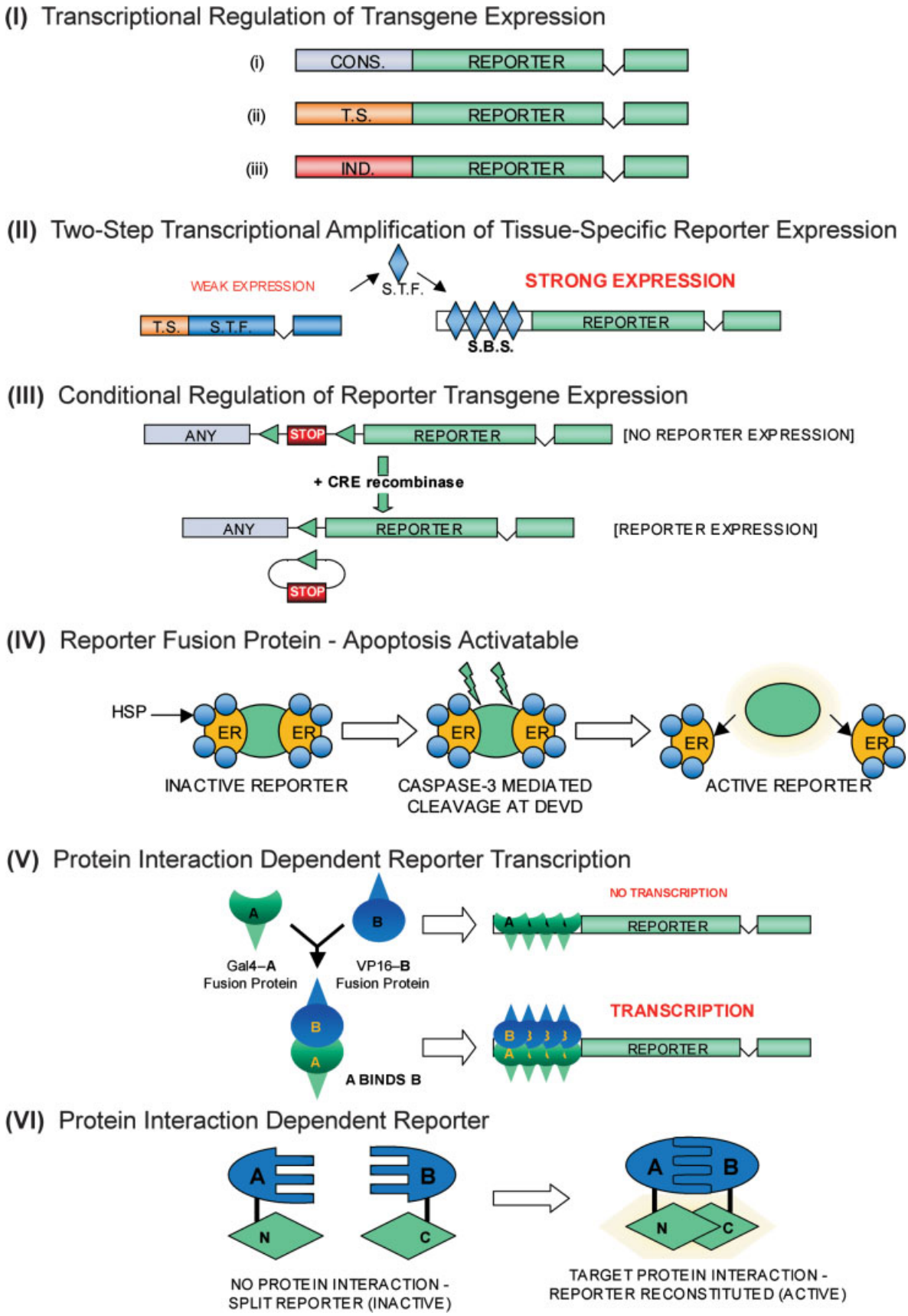

Figure 1. Reporter transgene strategies currently employed to non-invasively image tumour biology in mice. Please see main text and Table 2 for associated explanations and imaging applications. CONS = constitutive; T.S. = tissue-specific; IND = inducible; S.T.F. = synthetic transcription factor; S.B.S. = synthetic binding sites; HSP = heat-shock protein; ER = oestrogen receptor domain

Another approach, termed two-step transcriptional amplification (TSTA), can increase imaging sensitivity when relatively weak tissue-specific promoters are required to regulate reporter transgene expression [27]. As depicted in Figure 1 (II), two expression cassettes are involved. The first drives weak but tissue-specific expression of a synthetic and strong transcription factor (VP16-Gal4 fusion protein). The second construct comprises the reporter transgene of choice driven by a synthetic promoter containing multiple Gal4 binding sites. As the reporter transgene does not express in the absence of the VP16-Gal4 transcription factor, overall tissue specificity is maintained according to the promoter employed in the first construct. TSTA has been able to significantly amplify prostate-specific expression of both luciferase and HSV-TK reporter genes when using a modified PSA (prostate-specific antigen) promoter to weakly express VP16-Gal4 [27,28]. Beyond increasing the sensitivity of tissue-specific imaging, this approach may yet prove most useful for boosting tissue-specific expression levels of therapeutic transcripts delivered by gene therapy vectors [29]. To this end, a new bi-directional promoter has been developed that will enable the dual amplification of both reporter and therapeutic transgene expression simultaneously [30].

Conditional (Cre/loxP-dependent) activation of reporter transgene expression [Figure 1, (III)] has proven to be a successful strategy for imaging spontaneous tumourigenesis in a conditional mouse model of lung cancer (see Figure 2.4) [31]. This strategy can employ constitutive, tissue-specific or inducible promoters as desired; however, the reporter transgene does not express until Cre recombinase activity has removed a stop codon positioned between the promoter and the reporter. Cre expression is introduced through the germline in the majority of conditional mouse tumour models, but can also be introduced somatically using engineered viruses [32]. A conditional (Cre/loxP-dependent) HSV-TK allele has also been developed recently which should allow PET and SPECT imaging of conditional tumourigenesis in mice in the future [33].

Imaging other meaningful aspects of *in vivo* tumour biology has been achieved through the development of transgenic constructs that rely upon post-translational regulation of reporter transgene expression or functionality. For example, the induction of apoptosis has been imaged non-invasively *in vivo* via the use of a reporter transgene fused to oestrogen receptor (ER) domains via a stretch of amino acids containing the DEVD caspase-3 consensus motif [Figure 1, (IV)]. Under normal cellular conditions, bulky heat-shock proteins bind to the ER domains and sterically inhibit reporter transgene function. Apoptosis-induced caspase activity cleaves the ER domains from the reporter, essentially ensuring reporter functionality for the period of time that the cell remains viable [34]. The application of reporter fusion proteins comprising part reporter–part gene of interest is also facilitating the development of *in vivo* drug efficacy screens for specific classes of compound. A reporter–ubiquitin fusion protein strategy has led to the development of a non-invasive screen for compounds that inhibit proteasome activity *in vivo* [35] and another recently published study employed a reporter–p27 fusion protein to non-invasively screen compounds for *in vivo* Cdk2 inhibitory properties [36].

Fusion proteins have also been successfully employed to non-invasively image protein–protein interactions within living mice. One such approach, similar to a yeast two-hybrid screen, enabled the visualization of p53 interaction with SV40 T-antigen *in vivo* using PET [Figure 1, (V)]. p53 was fused to a Gal4 DNA-binding domain and T-antigen was fused to the VP16-transcriptional transactivation domain. Thus, the specific activation of reporter transgene expression, driven by a synthetic promoter containing multiple Gal4 binding sites, could only arise following p53–T-antigen interaction *in vivo* and the consequent reconstitution of synthetic transcription factor activity [37,38].

Protein–protein interactions within cells have also been non-invasively imaged using a split reporter transgene strategy. This strategy involves the fusion of N- and C-terminal fragments of a split reporter transgene onto either one of the interacting proteins to be visualized [Figure 1, (VI)]. These individual reporter fragments themselves are essentially dysfunctional; however, when protein–protein interaction occurs, reporter function is reconstituted. To date, this split-reporter approach has been developed for both *Renilla* and firefly luciferase transgenes and has been used to image Myo-D interaction with Id [39], rapamycin-mediated heterodimerization of FKB and FKBP12 [40], Cdc25C interaction with 14-3-3ε, and STAT1 homodimerization [41]. Imaging approaches such as these will undoubtedly prove invaluable for screening the ability of compounds to prevent specific clinically relevant protein–protein interactions *in vivo*.

Advances in MRI imaging

MRI is able to provide both high-resolution anatomical information and functional measurements of tumour physiology and so comprises one of the more versatile all-round modalities with which to image tumours in small animals. Most of the recent advances associated with this modality have come from the development of new MRI techniques and reagents that are able to non-invasively image diverse functional aspects of tumour physiology.

One way that MRI can measure various biological parameters is through the application of different types of imaging probe. Imaging probes for any modality can be classified in three ways: non-specific, targeted or activatable. All three classes of MRI probe typically contain a paramagnetic cation or nanosized particle and can be developed for both preclinical and clinical uses [12].

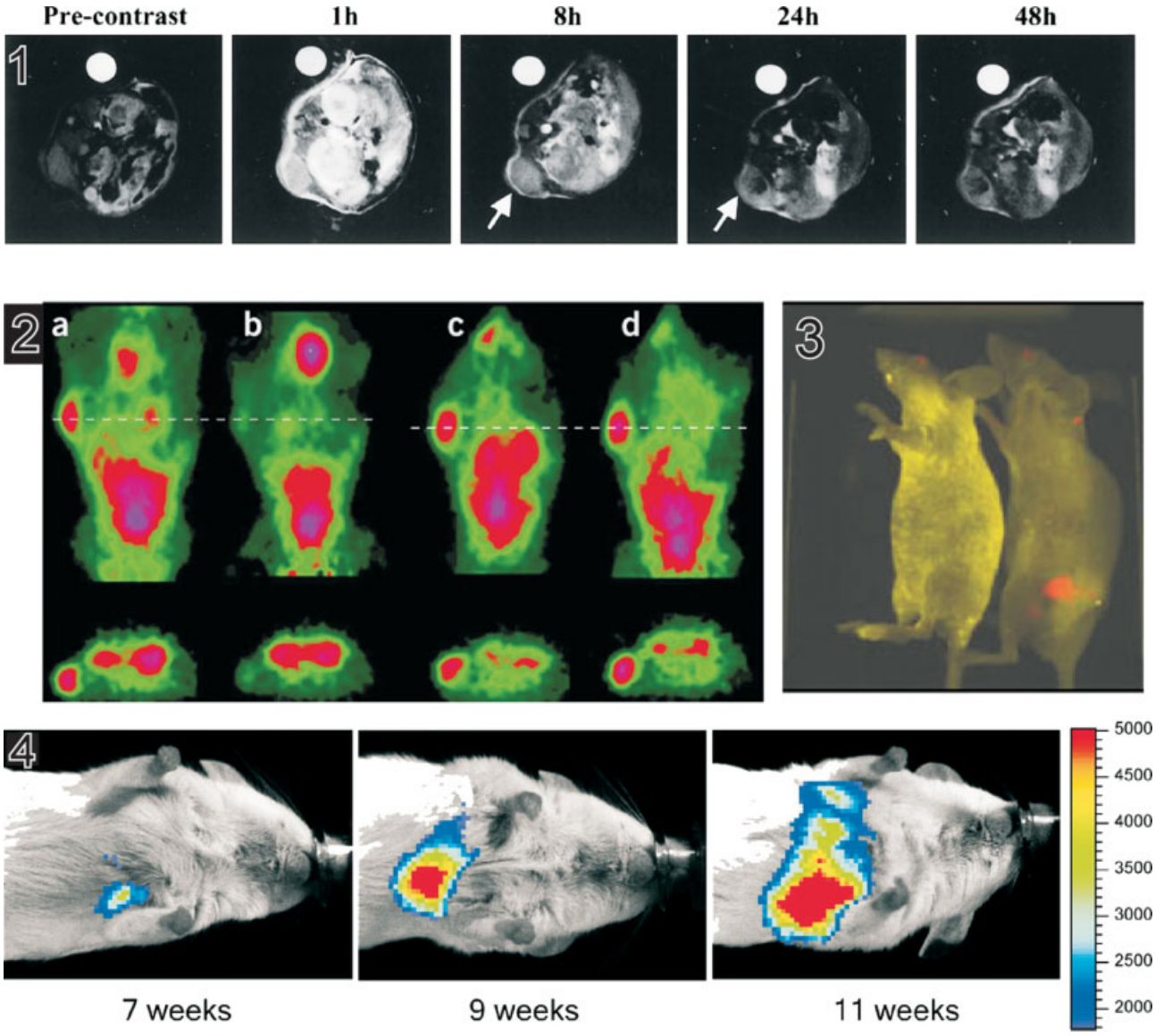

Figure 2. Examples of targeted or conditional tumour imaging in mice. Panels 1 depict magnetic resonance T1-weighted images of NT-5 tumours taken before administration of a targeted contrast agent (avidin–GdDTPA conjugate) and at 1, 8, 24, and 48 h after contrast. Arrows show enhanced signal from the HER-2/*neu*-expressing tumour at the 8 and 24 h time points [44]. Panel 2 (a–d) depicts micro-PET images (coronal slice and transverse slice through the tumour and kidneys) of two different nude mice with single BT-474 tumours. (a) A mouse at 3 h after injection with ^{68}Ga-DCHF (DOTA-conjugated herceptin fragment) and before 17-AAG treatment; (b) the same mouse after it had received 3 $\times$ 50 mg/kg 17-AAG and was rescanned 24 h later; (c, d) comparable images of a control mouse 3 h after one dose of ^{68}Ga-DCHF (c) and after a second dose 24 h later (d) [51]. Panel 3 depicts super-imposed spectral imaging (fluorescence imaging) of PSMA antibody-conjugated quantum dots in live animals harbouring C4-2 tumour xenografts. Orange-red fluorescence signals indicate a prostate tumour growing in a live mouse (right). Control studies using a healthy mouse (no tumour) and the same amount of QD injection showed no localized fluorescence signals (left) [87]. Panels 4 depict longitudinal BLI measurement of spontaneous *Kras2*^{v12}-induced lung tumour growth from conditional luciferase/conditional *Kras2*^{v12} compound mice. Images were taken at 2-week intervals and the number of weeks annotating each individual image refers to the time elapsed after intratracheal administration of adenoviral Cre [31]. Note that the colours on these images depict relative light intensity and do not represent actual coloured light. Figure 2.1 is reproduced with modification from Figure 3 in Artemov D, Mori N, Ravi R, Bhujwalla ZM, Magnetic resonance molecular imaging of the HER-2/neu receptor, *Cancer Res* 2003;**63**:2723–2727 by copyright permission of AACR. Figure 2.2 is reproduced with modification from Figure 3 in Smith-Jones PM, Solit DB, Akhurst T, Afroze F, Rosen N, Larson SM, Imaging the pharmacodynamics of HER2 degradation in response to Hsp90 inhibitors, *Nature Biotechnol* 2004;**22**:701–706 by copyright permission of Nature Publishing Group http://www.nature.com/ Figure 2.3 reproduced with modification from Figure 4 in Gao X, Cui Y, Levenson RM, Chung LW, Nie S, *In vivo* cancer targeting and imaging with semiconductor quantum dots, *Nature Biotechnol* 2004;**22**:969–976 by copyright permission of Nature Publishing Group http://www.nature.com/ Figure 2.4 is reproduced with modification from Figure 4 in Lyons SK, Meuwissen R, Krimpenfort P, Berns A, The generation of a conditional reporter that enables bioluminescence imaging of Cre/loxP-dependent tumorigenesis in mice, *Cancer Res* 2003;**63**:7042–7046 by copyright permission of AACR

Non-specific MRI probes passively accumulate in different tissue types and so can aid resolution of tumour margins from normal tissue [42]. In contrast, targeted probes specifically localize to defined cell types in tissue via internalization or interaction with proteins expressed on the surface of the target cell. For example, both an MRI probe [CLIO (cross-linked iron oxide)] and a near-infrared fluorochrome [Cy5.5 (cyanine 5.5)] could be targeted to tumours that overexpressed the tumour-specific antigen uMUC1 via the attachment of a short specific peptide sequence. Intravenous injection of this probe resulted in tumour-specific accumulation and enhanced detection of tumour burden *in vivo* via both MRI and optical imaging techniques [43]. Another study recently targeted a different MR contrast agent, gadolinium, to HER2/neu-expressing tumour cells *in vivo* via the development of a specific antibody conjugate (see Figure 2.1) [44]. Additionally, an iron oxide–transferrin chelate exhibited greatly enhanced accumulation in tumour cells that overexpressed transferrin receptor [45]. Activatable probes are only detectable following interaction with a specific molecular target and so can enable non-invasive imaging of molecular activity *in vivo*. One such activatable MRI probe is specifically activated in cells that express the marker transgene β-galactosidase [20].

The majority of MRI applications mentioned so far employ imaging techniques termed T1 or T2 relaxation imaging. Another technique, termed diffusion MRI, is currently being developed for its ability to predict the outcome of therapeutic intervention *in vivo* [46]. This method is able to detect relatively small changes in tissue structure by measuring the mobility of water and can characterize relatively acellular regions, indicative of positive therapeutic effect, from within fields of normal tissue. A further MR-based technique, termed magnetic resonance spectroscopy, has the ability to non-invasively differentiate tumour cell from normal cell metabolism on the basis of measured differences in intracellular hydrogen, carbon or phosphorus isotopes [47]. In addition to enabling non-invasive measurements of tumour progression, this approach can also be used to measure changes in tumour cell metabolism following the administration of different therapeutic agents, thereby contributing to our understanding of drug mechanism.

Advances in PET and SPECT imaging

Although PET and SPECT imaging approaches utilize different hardware and radioisotopes, both approaches are reliant upon the detection of γ-rays arising from radioisotope decay. PET imaging is one of the most sensitive imaging approaches and picomolar amounts of radiolabel can be readily detected and quantified *in vivo*, irrespective of tissue depth. This compares very favourably with the use of probes for SPECT and MRI, where 10^1-10^2 and 10^7-10^8 greater amounts of probe are required, respectively. In the past, a commonly used PET imaging probe was ^{18}F-labelled glucose, which achieved tumour-specific accumulation on the basis that tumour cells have a higher rate of glucose uptake and metabolism (glycolysis) than normal tissues [47]. Presently, many other PET and SPECT probes have been developed that passively confer tumour specificity via a variety of different tumour-specific mechanisms (for a recent list see ref 13).

The development of targeted radiolabelled ligands has further enabled both SPECT and PET to image diverse aspects of *in vivo* tumour biology. Radiolabelled annexin V, for example, has been used to non-invasively detect tumour cell apoptosis *in vivo* following chemotherapy via its interaction with extracellular phosphatidylserine, a hallmark of apoptosis [48]. Radiolabel can also be targeted to angiogenic blood vessels in tumours *in vivo* by exploiting the affinity of small peptides containing the amino acids RGD with $\alpha_v\beta_3$ integrin [49,50].

The pharmacokinetics and pharmacodynamics of radiolabelled anti-cancer therapeutics can, in principle, also be monitored by these methods and so lead to rapid improvements in drug scheduling or design. The effects of 17-AAG treatment on HER2 expression levels in a tumour have been measured non-invasively over time by PET, following the conjugation of an $F(ab')_2$ fragment derived from the anti-HER2 antibody herceptin with ^{68}Ga (see Figure 2.2) [51]. The biodistribution and metabolism of labelled 5-FU, as well as an antibody raised against vascular endothelial growth factor (VEGF), have also been imaged by PET or SPECT in mice [52,53].

As mentioned in a previous section, probes have also been developed for PET and SPECT that accumulate specifically in transgene-expressing cells. One of the transgenes most commonly used for such purposes is thymidine kinase from herpes simplex virus (HSV-TK), which specifically phosphorylates trace amounts of radiolabelled nucleoside analogues [such as FIAU (2′-fluoro-2′-deoxy-1-β-D-arabinofuranosyl-5-iodouracil) or gancyclovir], leading to their incorporation into the DNA of replicating cells. A modified form of HSV-TK has also been developed (termed HSV-TKser39) that has greater activity relative to wild type and so is further able to enhance imaging sensitivity [54].

HSV-TK-based approaches have enabled both the quantitative and the tomographic measurement of adenoviral and lentiviral gene transduction *in vivo* by PET [55,56]. Non-invasive visualization of cellular immunotherapy has also been achieved using HSV-TK-labelled T-cells, which were seen to migrate to sites of tumour development in mice [57,58]. Furthermore, specific aspects of tumour physiology have been measured with PET, including hypoxia (HIF-1α regulated HSV-TK) [25] and p53-dependent transcription of an HSV-TK/GFP fusion protein in response to genotoxic stress [26]. Other transgenes

(and their respective radiolabelled probes) validated for tumour imaging with PET or SPECT include the dopamine D2 receptor, somatostatin-2 receptor and NIS (sodium-iodine symporter) [59]. The latter, NIS, was recently used to non-invasively measure human telomerase promoter activity in tumour cells *in vivo* by PET [60].

Advances in optical bioluminescence imaging

The luciferase from two species, the sea-pansy (*Renilla reniformis*) and the North American firefly (*Photinus pyralis*), has been commonly used to label and image tumour cells in mice [61]. As with other optical-based *in vivo* imaging approaches, this approach is reliant upon the detection of light emission from within living tissues. Unlike fluorescence imaging, however, light emission does not first require excitation of the reporter, but instead arises from substrate catalysis [luciferin in the case of firefly luciferase (Fluc) and coelenterazine in the case of *Renilla* luciferase (Rluc)].

To date, Fluc has been more extensively used for *in vivo* imaging than Rluc, partly because Fluc emits proportionally more red-shifted light, which has better tissue penetrance properties than the predominantly blue-green emission of Rluc [62]. A new codon-modified version of Rluc (termed hRluc) has recently been developed, however, and used in several *in vivo* tumour cell-imaging studies [62,63]. This synthetic version of Rluc is reportedly better expressed in mammalian cells and emits light with a greater intensity relative to the original native Rluc enzyme.

Constitutive expression of luciferase has rendered many different xenograft tumour cell lines stably bioluminescent. Tight correlations have been demonstrated between photon emission and tumour burden and so the growth of primary tumours and spontaneous metastases can be quantified non-invasively, even when arising at deep-tissue sites [5,21,24,64]. As with fluorescence techniques, deeper sources of light are prone to greater degrees of signal attenuation (ie a population of luciferase-expressing cells near the surface of the skin will appear brighter than the same number of cells growing at deeper tissue sites such as the liver or lung). Therefore, although not an absolutely quantitative imaging approach like PET (γ-rays are not attenuated passing through tissue), the growth dynamics of tumours or metastases can be accurately determined by quantifying the relative change in light emission intensity over time.

Fluc is also proving to be a particularly useful marker for measuring the efficacy of cancer therapeutics. ATP and oxygen are required in addition to luciferin substrate for light emission; therefore Fluc provides a quantitative measure of viable cells only [8,64,65]. Image acquisition times are also typically short, often ranging from 1 to 60 s, making it possible to evaluate several treatment cohorts in a single imaging session.

Tumour cells can be dual-labelled with Rluc and Fluc and imaged sequentially with the same hardware, as the substrates for these markers do not cross-react [66]. The advantages of dual-labelling were recently exemplified in a study whereby human glioma tumour cell burden was quantified non-invasively using Fluc, whilst the efficiency of tumour cell transduction by a therapeutic virus was simultaneously measured using Rluc [67]. As both of these parameters could be repeatedly measured in a living animal, the efficiency of gene delivery could be directly correlated with the efficacy of the therapeutic approach over time.

Rluc may not prove to be ideally suited for imaging all tumour models, however, as it has been recently shown that its substrate, coelenterazine, is actively transported out of cells by the MDR1 P-glycoprotein [68]. Consequently, Rluc-labelled cells have been effectively used to screen the activity of MDR1 inhibitors *in vivo*. However, as light emission increases from Rluc-labelled cells following inhibition of MDR1 function, Rluc is unlikely to comprise the most sensitive means to image other biological parameters in tumour cells that overexpress MDR1.

Advances in optical fluorescence imaging

Tumours in mice can also be imaged *in vivo* by fluorescence imaging techniques when labelled with fluorescent proteins, dyes or nanosized photonic crystals termed 'quantum dots'. Light emission from labelled cells first requires excitation of the fluorescent marker with relatively shorter wavelengths of light. As with BLI, wavelengths of light greater than 600 nm are less susceptible to absorbance by surrounding tissue; thus, fluorescent materials that emit far-red and near-infrared light are preferable when imaging at non-superficial sites in the mouse [69]. The imaging sensitivity of far-red and near-infrared materials is further enhanced by the fact that their excitation results in significantly reduced levels of autofluorescence from normal non-labelled tissues.

Fluorescent labels have proven to be a highly versatile means with which to image tumours in mice, as in addition to providing an opportunity to observe tumour biology *in vivo*, labelled cells are particularly well suited to *ex vivo* analyses (eg fluorescence microscopy or FACS analysis) once experimental end-points have been reached [22,70,71].

Constitutively expressed fluorescent proteins have been used as a transgenic marker to non-invasively image primary tumour development and metastases [72], and also comprise a useful means with which to visualize somatic gene transfer from therapeutic vectors [73]. Different fluorescent proteins with distinct excitation and emission wavelength properties have been simultaneously expressed in mice to investigate *in vivo* interactions between tumour and stroma. One such dual-labelling approach grew red fluorescent protein (RFP)-labelled tumours in green fluorescent protein (GFP)-labelled recipient mice and could

differentiate whether cells were of tumour or stromal origin in fresh-tissue biopsy [22]. Populations of tumour cells labelled with either GFP or RFP have also been imaged together to investigate the clonal nature of metastasis [74]. And another tumour model, partly comprised of a transgenic mouse with VEGF promoter regulated GFP, showed specific induction of VEGF expression from surrounding stromal tissue in response to tumour stimulation [75].

Tumour cells can also be fluorescently labelled *in vivo* with specifically targeted or activatable fluorescent imaging probes. A wide range of fluorescent materials are available that emit light in all portions of the visible spectrum [69]; however, many recent imaging studies have employed far-red and rear-infrared emitting fluorochromes (ie Cy5.5) to improve tissue penetrance of signal and reduce autofluorescence. For example, Cy5.5 has been used in one study to label epithelial growth factor (EGF) and so image EGF receptor expression in breast tumours [76]. Another study used Cy5.5-labelled endostatin to show its specific accumulation in tumour vasculature following intraperitoneal injection [77], and a Cy5.5-short peptide conjugate has also been specifically targeted to intestinal tumours in mice and visualized *in vivo* using a miniaturized fibre-optic endoscope [78]. Other imaging probes have been developed that only fluoresce following activation by *in vivo* protease activity [79–82], or by a marker commonly associated with tumour malignancy [83].

Quantum dots (QDs) comprise a new fluorescent label that has great potential to image multiple biological processes concurrently within tumours growing *in vivo*. These nanosized particles fluoresce brightly when excited and possess tight, highly specific emission wavelength properties (ranging from visible to near-infrared portions of the spectrum) that are directly proportional to the size of their photo-excitable core. QD cores are typically composed of CdSe or CdTe, which are encased in an inert protective shell and a layer of material that enables direct conjugation of the dot to other macromolecules including antibodies, streptavidin or nucleic acids. The parameters defining optimal *in vivo* imaging conditions for QDs continue to evolve and improve [84,85]. However, QDs have so far been targeted to tumour-specific targets such as HER2 or PSMA (prostate-specific membrane antigen) using antibody conjugates (see Figure 2.3) [86,87], and to specific organs such as the lungs, tumour-associated vasculature, and lymph in living mice using short peptide conjugates [88]. It seems likely that the variety of available QD colours coupled with the ability to conjugate these dots to a diverse array of macromolecules will soon ensure non-invasive multiplex imaging *in vivo*. QDs may also find future clinical applications, as near-infrared dots have been used to map sentinel lymph nodes in pigs prior to and during resection [89].

Currently, most *in vivo* fluorescence imaging approaches employ 'planar' detection of fluorescent light. The collection of fluorescent signal from three dimensions has resulted in the development of a new tomographic fluorescence imaging method termed FMT (fluorescence molecular tomography) [90]. The overall utility and improved signal quantification of FMT were recently demonstrated in a study measuring *in vivo* tumour cell apoptosis following chemotherapy [91].

Fluorescently labelled cells can also be imaged at very high resolution *in vivo*, following the introduction of a small surgical 'window' into tissues overlying the tumour, using a modified fluorescence microscope in an approach termed intra-vital microscopy [92].

One such intra-vital imaging approach, employing laser-scanning microscopy and multi-photon excitation, is now advancing our fundamental understanding of tumour cell metastasis via direct, real-time *in vivo* observations of primary tumour cell interaction with the extracellular matrix and micro-vasculature [93].

Conclusions

The continued refinement and increased availability of small animal imaging modalities have recently led to rapid progress in the variety of ways that tumour biology can be visualized non-invasively in living mice.

These advances are set to benefit cancer patients in multiple ways. Longitudinal tumour analyses can provide new insights into basic tumour biology, which will potentially lead to the identification of new molecular targets or treatment strategies. Functional imaging probes applicable for use with clinical imaging modalities can now also be developed and optimized preclinically with murine tumour models. The development of such probes should ultimately improve our ability to detect tumours in humans, as well as to non-invasively monitor surrogate biomarkers indicative of positive therapeutic response following their treatment.

Current small animal imaging techniques now also facilitate the use of spontaneous tumour models for treatment evaluation, likely resulting in the improved stringency and predictiveness of preclinical testing [94]. Furthermore, the quality of data collected from preclinical drug efficacy trials should also greatly improve and expedite the optimization of administrative dose scheduling and drug chemistry, as well as help to demonstrate positive synergistic effects arising from combinations of treatments *in vivo*.

Taken together, small animal imaging approaches are now beginning to significantly increase the overall utility of mouse tumour models in the laboratory, which in turn should result in improved clinical practices.

Acknowledgements

I would like to thank John Hunter, David Boyko, Brad Rice, Darlene Jenkins, and Tony Purchio for providing critical and

insightful comments, and Joycelyn Bishop for assistance in formatting this manuscript.

References

1. Aguirre AJ, Bardeesy N, Sinha M, *et al*. Activated Kras and Ink4a/Arf deficiency cooperate to produce metastatic pancreatic ductal adenocarcinoma. *Genes Dev* 2003; **17**: 3112–3126.
2. Krimpenfort P, Quon KC, Mooi WJ, Loonstra A, Berns A. Loss of p16Ink4a confers susceptibility to metastatic melanoma in mice. *Nature* 2001; **413**: 83–86.
3. Wang S, Gao J, Lei Q, *et al*. Prostate-specific deletion of the murine Pten tumor suppressor gene leads to metastatic prostate cancer. *Cancer Cell* 2003; **4**: 209–221.
4. Artandi SE, Chang S, Lee SL, *et al*. Telomere dysfunction promotes non-reciprocal translocations and epithelial cancers in mice. *Nature* 2000; **406**: 641–645.
5. Douma S, Van Laar T, Zevenhoven J, Meuwissen R, Van Garderen E, Peeper DS. Suppression of anoikis and induction of metastasis by the neurotrophic receptor TrkB. *Nature* 2004; **430**: 1034–1039.
6. Bergers G, Javaherian K, Lo KM, Folkman J, Hanahan D. Effects of angiogenesis inhibitors on multistage carcinogenesis in mice. *Science* 1999; **284**: 808–812.
7. Satchi-Fainaro R, Puder M, Davies JW, *et al*. Targeting angiogenesis with a conjugate of HPMA copolymer and TNP-470. *Nature Med* 2004; **10**: 255–261.
8. Shah NP, Tran C, Lee FY, Chen P, Norris D, Sawyers CL. Overriding imatinib resistance with a novel ABL kinase inhibitor. *Science* 2004; **305**: 399–401.
9. Romer JT, Kimura H, Magdaleno S, *et al*. Suppression of the Shh pathway using a small molecule inhibitor eliminates medulloblastoma in Ptc1(+/−) p53(−/−) mice. *Cancer Cell* 2004; **6**: 229–240.
10. Schmitt CA, Fridman JS, Yang M, Baranov E, Hoffman RM, Lowe SW. Dissecting p53 tumor suppressor functions *in vivo*. *Cancer Cell* 2002; **1**: 289–298.
11. Wendel HG, De Stanchina E, Fridman JS, *et al*. Survival signalling by Akt and eIF4E in oncogenesis and cancer therapy. *Nature* 2004; **428**: 332–337.
12. Weissleder R. Scaling down imaging: molecular mapping of cancer in mice. *Nature Rev Cancer* 2002; **2**: 11–18.
13. Massoud TF, Gambhir SS. Molecular imaging in living subjects: seeing fundamental biological processes in a new light. *Genes Dev* 2003; **17**: 545–580.
14. Goertzen AL, Meadors AK, Silverman RW, Cherry SR. Simultaneous molecular and anatomical imaging of the mouse *in vivo*. *Phys Med Biol* 2002; **47**: 4315–4328.
15. Rehemtulla A, Hall DE, Stegman LD, *et al*. Molecular imaging of gene expression and efficacy following adenoviral-mediated brain tumor gene therapy. *Mol Imaging* 2002; **1**: 43–55.
16. Ray P, De A, Min JJ, Tsien RY, Gambhir SS. Imaging tri-fusion multimodality reporter gene expression in living subjects. *Cancer Res* 2004; **64**: 1323–1330.
17. Ponomarev V, Doubrovin M, Serganova I, *et al*. A novel triple-modality reporter gene for whole-body fluorescent, bioluminescent, and nuclear noninvasive imaging. *Eur J Nucl Med Mol Imaging* 2004; **31**: 740–751.
18. Ichikawa T, Hogemann D, Saeki Y, *et al*. MRI of transgene expression: correlation to therapeutic gene expression. *Neoplasia* 2002; **4**: 523–530.
19. Tung CH, Zeng Q, Shah K, Kim DE, Schellingerhout D, Weissleder R. *In vivo* imaging of beta-galactosidase activity using far red fluorescent switch. *Cancer Res* 2004; **64**: 1579–1583.
20. Louie AY, Huber MM, Ahrens ET, *et al*. *In vivo* visualization of gene expression using magnetic resonance imaging. *Nature Biotechnol* 2000; **18**: 321–325.
21. Jenkins DE, Oei Y, Hornig YS, *et al*. Bioluminescent imaging (BLI) to improve and refine traditional murine models of tumor growth and metastasis. *Clin Exp Metastasis* 2003; **20**: 733–744.
22. Yang M, Li L, Jiang P, Moossa AR, Penman S, Hoffman RM. Dual-color fluorescence imaging distinguishes tumor cells from induced host angiogenic vessels and stromal cells. *Proc Natl Acad Sci U S A* 2003; **100**: 14 259–14 262.
23. Adams JY, Johnson M, Sato M, *et al*. Visualization of advanced human prostate cancer lesions in living mice by a targeted gene transfer vector and optical imaging. *Nature Med* 2002; **8**: 891–897.
24. Vooijs M, Jonkers J, Lyons S, Berns A. Noninvasive imaging of spontaneous retinoblastoma pathway-dependent tumors in mice. *Cancer Res* 2002; **62**: 1862–1867.
25. Serganova I, Doubrovin M, Vider J, *et al*. Molecular imaging of temporal dynamics and spatial heterogeneity of hypoxia-inducible factor-1 signal transduction activity in tumors in living mice. *Cancer Res* 2004; **64**: 6101–6108.
26. Doubrovin M, Ponomarev V, Beresten T, *et al*. Imaging transcriptional regulation of p53-dependent genes with positron emission tomography *in vivo*. *Proc Natl Acad Sci U S A* 2001; **98**: 9300–9305.
27. Iyer M, Wu L, Carey M, Wang Y, Smallwood A, Gambhir SS. Two-step transcriptional amplification as a method for imaging reporter gene expression using weak promoters. *Proc Natl Acad Sci U S A* 2001; **98**: 14 595–14 600.
28. Sato M, Johnson M, Zhang L, *et al*. Optimization of adenoviral vectors to direct highly amplified prostate-specific expression for imaging and gene therapy. *Mol Ther* 2003; **8**: 726–737.
29. Iyer M, Salazar FB, Lewis X, *et al*. Noninvasive imaging of enhanced prostate-specific gene expression using a two-step transcriptional amplification-based lentivirus vector. *Mol Ther* 2004; **10**: 545–552.
30. Ray S, Paulmurugan R, Hildebrandt I, *et al*. Novel bidirectional vector strategy for amplification of therapeutic and reporter gene expression. *Hum Gene Ther* 2004; **15**: 681–690.
31. Lyons SK, Meuwissen R, Krimpenfort P, Berns A. The generation of a conditional reporter that enables bioluminescence imaging of Cre/loxP-dependent tumorigenesis in mice. *Cancer Res* 2003; **63**: 7042–7046.
32. Jonkers J, Berns A. Conditional mouse models of sporadic cancer. *Nature Rev Cancer* 2002; **2**: 251–265.
33. Sundaresan G, Paulmurugan R, Berger F, *et al*. MicroPET imaging of Cre-loxP-mediated conditional activation of a herpes simplex virus type 1 thymidine kinase reporter gene. *Gene Ther* 2004; **11**: 609–618.
34. Laxman B, Hall DE, Bhojani MS, *et al*. Noninvasive real-time imaging of apoptosis. *Proc Natl Acad Sci U S A* 2002; **99**: 16 551–16 555.
35. Luker GD, Pica CM, Song J, Luker KE, Piwnica-Worms D. Imaging 26S proteasome activity and inhibition in living mice. *Nature Med* 2003; **9**: 969–973.
36. Zhang GJ, Safran M, Wei W, *et al*. Bioluminescent imaging of Cdk2 inhibition *in vivo*. *Nature Med* 2004; **10**: 643–648.
37. Luker GD, Sharma V, Pica CM, *et al*. Noninvasive imaging of protein–protein interactions in living animals. *Proc Natl Acad Sci U S A* 2002; **99**: 6961–6966.
38. Luker GD, Sharma V, Pica CM, Prior JL, Li W, Piwnica-Worms D. Molecular imaging of protein–protein interactions: controlled expression of p53 and large T-antigen fusion proteins *in vivo*. *Cancer Res* 2003; **63**: 1780–1788.
39. Paulmurugan R, Umezawa Y, Gambhir SS. Noninvasive imaging of protein–protein interactions in living subjects by using reporter protein complementation and reconstitution strategies. *Proc Natl Acad Sci U S A* 2002; **99**: 15 608–15 613.
40. Paulmurugan R, Massoud TF, Huang J, Gambhir SS. Molecular imaging of drug-modulated protein–protein interactions in living subjects. *Cancer Res* 2004; **64**: 2113–2119.
41. Luker KE, Piwnica-Worms D. Optimizing luciferase protein fragment complementation for bioluminescent imaging of protein–protein interactions in live cells and animals. *Methods Enzymol* 2004; **385**: 349–360.
42. Moffat BA, Reddy GR, McConville P, *et al*. A novel polyacrylamide magnetic nanoparticle contrast agent for molecular imaging using MRI. *Mol Imaging* 2003; **2**: 324–332.

43. Moore A, Medarova Z, Potthast A, Dai G. *In vivo* targeting of underglycosylated MUC-1 tumor antigen using a multimodal imaging probe. *Cancer Res* 2004; **64**: 1821–1827.
44. Artemov D, Mori N, Ravi R, Bhujwalla ZM. Magnetic resonance molecular imaging of the HER-2/neu receptor. *Cancer Res* 2003; **63**: 2723–2727.
45. Weissleder R, Moore A, Mahmood U, *et al*. *In vivo* magnetic resonance imaging of transgene expression. *Nature Med* 2000; **6**: 351–355.
46. Ross BD, Moffat BA, Lawrence TS, *et al*. Evaluation of cancer therapy using diffusion magnetic resonance imaging. *Mol Cancer Ther* 2003; **2**: 581–587.
47. Griffin JL, Shockcor JP. Metabolic profiles of cancer cells. *Nature Rev Cancer* 2004; **4**: 551–561.
48. Mandl SJ, Mari C, Edinger M, *et al*. Multi-modality imaging identifies key times for annexin V imaging as an early predictor of therapeutic outcome. *Mol Imaging* 2004; **3**: 1–8.
49. Janssen ML, Oyen WJ, Dijkgraaf I, *et al*. Tumor targeting with radiolabeled alpha(v)beta(3) integrin binding peptides in a nude mouse model. *Cancer Res* 2002; **62**: 6146–6151.
50. Chen X, Liu S, Hou Y, *et al*. MicroPET imaging of breast cancer alpha(v)-integrin expression with (64)Cu-labeled dimeric RGD peptides. *Mol Imaging Biol* 2004; **6**: 350–359.
51. Smith-Jones PM, Solit DB, Akhurst T, Afroze F, Rosen N, Larson SM. Imaging the pharmacodynamics of HER2 degradation in response to Hsp90 inhibitors. *Nature Biotechnol* 2004; **22**: 701–706.
52. Visser GW, van der Wilt CL, Wedzinga R, Peters GJ, Herscheid JD. 18F-radiopharmacokinetics of [18F]-5-fluorouracil in a mouse bearing two colon tumors with a different 5-fluorouracil sensitivity: a study for a correlation with oncological results. *Nucl Med Biol* 1996; **23**: 333–342.
53. Collingridge DR, Carroll VA, Glaser M, *et al*. The development of [(124)I]iodinated-VG76e: a novel tracer for imaging vascular endothelial growth factor *in vivo* using positron emission tomography. *Cancer Res* 2002; **62**: 5912–5919.
54. Gambhir SS, Bauer E, Black ME, *et al*. A mutant herpes simplex virus type 1 thymidine kinase reporter gene shows improved sensitivity for imaging reporter gene expression with positron emission tomography. *Proc Natl Acad Sci U S A* 2000; **97**: 2785–2790.
55. Gambhir SS, Barrio JR, Phelps ME, *et al*. Imaging adenoviral-directed reporter gene expression in living animals with positron emission tomography. *Proc Natl Acad Sci U S A* 1999; **96**: 2333–2338.
56. De A, Lewis XZ, Gambhir SS. Noninvasive imaging of lentiviral-mediated reporter gene expression in living mice. *Mol Ther* 2003; **7**: 681–691.
57. Dubey P, Su H, Adonai N, *et al*. Quantitative imaging of the T cell antitumor response by positron-emission tomography. *Proc Natl Acad Sci U S A* 2003; **100**: 1232–1237.
58. Koehne G, Doubrovin M, Doubrovina E, *et al*. Serial *in vivo* imaging of the targeted migration of human HSV-TK-transduced antigen-specific lymphocytes. *Nature Biotechnol* 2003; **21**: 405–413.
59. Sharma V, Luker GD, Piwnica-Worms D. Molecular imaging of gene expression and protein function *in vivo* with PET and SPECT. *J Magn Reson Imaging* 2002; **16**: 336–351.
60. Groot-Wassink T, Aboagye EO, Wang Y, Lemoine NR, Keith WN, Vassaux G. Noninvasive imaging of the transcriptional activities of human telomerase promoter fragments in mice. *Cancer Res* 2004; **64**: 4906–4911.
61. Contag CH, Ross BD. It's not just about anatomy: *in vivo* bioluminescence imaging as an eyepiece into biology. *J Magn Reson Imaging* 2002; **16**: 378–387.
62. Bhaumik S, Walls Z, Puttaraju M, Mitchell LG, Gambhir SS. Molecular imaging of gene expression in living subjects by spliceosome-mediated RNA trans-splicing. *Proc Natl Acad Sci U S A* 2004; **101**: 8693–8698.
63. Massoud TF, Paulmurugan R, Gambhir SS. Molecular imaging of homodimeric protein–protein interactions in living subjects. *FASEB J* 2004; **18**: 1105–1107.
64. Jenkins DE, Yu SF, Hornig YS, Purchio T, Contag PR. *In vivo* monitoring of tumor relapse and metastasis using bioluminescent PC-3M-luc-C6 cells in murine models of human prostate cancer. *Clin Exp Metastasis* 2003; **20**: 745–756.
65. Rehemtulla A, Stegman LD, Cardozo SJ, *et al*. Rapid and quantitative assessment of cancer treatment response using *in vivo* bioluminescence imaging. *Neoplasia* 2000; **2**: 491–495.
66. Bhaumik S, Gambhir SS. Optical imaging of *Renilla* luciferase reporter gene expression in living mice. *Proc Natl Acad Sci U S A* 2002; **99**: 377–382.
67. Shah K, Tang Y, Breakefield X, Weissleder R. Real-time imaging of TRAIL-induced apoptosis of glioma tumors *in vivo*. *Oncogene* 2003; **22**: 6865–6872.
68. Pichler A, Prior JL, Piwnica-Worms D. Imaging reversal of multidrug resistance in living mice with bioluminescence: MDR1 P-glycoprotein transports coelenterazine. *Proc Natl Acad Sci U S A* 2004; **101**: 1702–1707.
69. Troy T, Jekic-McMullen D, Sambucetti L, Rice B. Quantitative comparison of the sensitivity of detection of fluorescent and bioluminescent reporters in animal models. *Mol Imaging* 2004; **3**: 9–23.
70. Schmitt CA, Fridman JS, Yang M, *et al*. A senescence program controlled by p53 and p16INK4a contributes to the outcome of cancer therapy. *Cell* 2002; **109**: 335–346.
71. Joyce JA, Baruch A, Chehade K, *et al*. Cathepsin cysteine proteases are effectors of invasive growth and angiogenesis during multistage tumorigenesis. *Cancer Cell* 2004; **5**: 443–453.
72. Yang M, Baranov E, Jiang P, *et al*. Whole-body optical imaging of green fluorescent protein-expressing tumors and metastases. *Proc Natl Acad Sci U S A* 2000; **97**: 1206–1211.
73. Mahasreshti PJ, Kataram M, Wang MH, *et al*. Intravenous delivery of adenovirus-mediated soluble FLT-1 results in liver toxicity. *Clin Cancer Res* 2003; **9**: 2701–2710.
74. Yamamoto N, Yang M, Jiang P, *et al*. Determination of clonality of metastasis by cell-specific color-coded fluorescent-protein imaging. *Cancer Res* 2003; **63**: 7785–7790.
75. Fukumura D, Xavier R, Sugiura T, *et al*. Tumor induction of VEGF promoter activity in stromal cells. *Cell* 1998; **94**: 715–725.
76. Ke S, Wen X, Gurfinkel M, *et al*. Near-infrared optical imaging of epidermal growth factor receptor in breast cancer xenografts. *Cancer Res* 2003; **63**: 7870–7875.
77. Citrin D, Scott T, Sproull M, Menard C, Tofilon PJ, Camphausen K. *In vivo* tumor imaging using a near-infrared-labeled endostatin molecule. *Int J Radiat Oncol Biol Phys* 2004; **58**: 536–541.
78. Kelly K, Alencar H, Funovics M, Mahmood U, Weissleder R. Detection of invasive colon cancer using a novel, targeted, library-derived fluorescent peptide. *Cancer Res* 2004; **64**: 6247–6251.
79. Bremer C, Tung CH, Weissleder R. *In vivo* molecular target assessment of matrix metalloproteinase inhibition. *Nature Med* 2001; **7**: 743–748.
80. Marten K, Bremer C, Khazaie K, *et al*. Detection of dysplastic intestinal adenomas using enzyme-sensing molecular beacons in mice. *Gastroenterology* 2002; **122**: 406–414.
81. Messerli SM, Prabhakar S, Tang Y, *et al*. A novel method for imaging apoptosis using a caspase-1 near-infrared fluorescent probe. *Neoplasia* 2004; **6**: 95–105.
82. Shah K, Tung CH, Chang CH, *et al*. *In vivo* imaging of HIV protease activity in amplicon vector-transduced gliomas. *Cancer Res* 2004; **64**: 273–278.
83. Law B, Curino A, Bugge TH, Weissleder R, Tung CH. Design, synthesis, and characterization of urokinase plasminogen-activator-sensitive near-infrared reporter. *Chem Biol* 2004; **11**: 99–106.
84. Larson DR, Zipfel WR, Williams RM, *et al*. Water-soluble quantum dots for multiphoton fluorescence imaging *in vivo*. *Science* 2003; **300**: 1434–1436.
85. Ballou B, Lagerholm BC, Ernst LA, Bruchez MP, Waggoner AS. Noninvasive imaging of quantum dots in mice. *Bioconjug Chem* 2004; **15**: 79–86.
86. Wu X, Liu H, Liu J, *et al*. Immunofluorescent labeling of cancer marker Her2 and other cellular targets with semiconductor quantum dots. *Nature Biotechnol* 2003; **21**: 41–46.

87. Gao X, Cui Y, Levenson RM, Chung LW, Nie S. *In vivo* cancer targeting and imaging with semiconductor quantum dots. *Nature Biotechnol* 2004; **22**: 969–976.
88. Akerman ME, Chan WC, Laakkonen P, Bhatia SN, Ruoslahti E. Nanocrystal targeting *in vivo*. *Proc Natl Acad Sci U S A* 2002; **99**: 12 617–12 621.
89. Kim S, Lim YT, Soltesz EG, *et al*. Near-infrared fluorescent type II quantum dots for sentinel lymph node mapping. *Nature Biotechnol* 2004; **22**: 93–97.
90. Graves EE, Weissleder R, Ntziachristos V. Fluorescence molecular imaging of small animal tumor models. *Curr Mol Med* 2004; **4**: 419–430.
91. Ntziachristos V, Schellenberger EA, Ripoll J, *et al*. Visualization of antitumor treatment by means of fluorescence molecular tomography with an annexin V–Cy5.5 conjugate. *Proc Natl Acad Sci U S A* 2004; **101**: 12 294–12 299.
92. Jain RK, Munn LL, Fukumura D. Dissecting tumour pathophysiology using intravital microscopy. *Nature Rev Cancer* 2002; **2**: 266–276.
93. Condeelis J, Segall JE. Intravital imaging of cell movement in tumours. *Nature Rev Cancer* 2003; **3**: 921–930.
94. Holland EC. Mouse models of human cancer as tools in drug development. *Cancer Cell* 2004; **6**: 197–198.